Impulsive Noise Suppression and Background Normalization of Electrocardiogram Signals Using Morphological Operators

CHEE-HUNG HENRY CHU, MEMBER, IEEE, AND EDWARD J. DELP, SENIOR MEMBER, IEEE

Abstract—**A new approach to impulsive noise suppression and background normalization of digitized electrocardiogram signals is presented using mathematical morphological operators that incorporate the shape information of a signal. A brief introduction to these nonlinear signal processing operators, as well as a detailed description of the new algorithm, is presented. Empirical results show that the new algorithm has good performance in impulsive noise suppression and background normalization.**

I. Introduction

A new approach to impulsive noise suppression and background normalization of digitized EKG signals is presented in this paper. EKG signals are frequently plagued by impulsive noise, e.g., due to muscle activities and power line interference [1]. Moreover, background normalization is needed to correct the baseline drift of the signal caused by the respiration and motion of the subject [2]. Noise suppression is typically the first step performed in the processing of EKG signals [3]. It is important to limit the distortion of the EKG signal caused by the noise suppression algorithms before such tasks as *QRS* detection or temporal alignment can be performed. One of the objectives is to produce an output that can facilitate the detection of the *QRS* waves by computers; hence, of primary importance is preservation of the main *QRS* complex. Other applications include real-time processing of EKG signals acquired in "hostile" environments such as in ambulances or on board spacecraft. We note that issues such as artifact suppression and preserving the subtle notches and slurs in individual waves are significant for clinical diagnostics use.

The most common approach to noise suppression is by low-pass filtering [4], [5], which is ineffective for reducing impulsive noise. Since baseline drift is assumed to have relatively low frequency, baseline correction is typically performed by high-pass filtering the EKG data [6]. Effective alternatives to conventional linear filtering, particularly when dealing with impulsive noise, are nonlinear operators such as median filtering [7] or other ranked ordering methods [8]. This paper presents new algorithms that make use of a class of nonlinear signal processing operators, known as mathematical morphology, for processing EKG data. Morphological operators have been used in the field of image processing and are known for their robust performance in preserving the shape of a signal while suppressing noise [9]. An introduction to the morphological operators is given in Section II. The new algorithm is described in Section III. Experimental results addressing various aspects of the problem are presented in Sections IV–VIII.

Manuscript received January 20, 1988; revised September 19, 1988. This work was supported in part by the Showalter Foundation.

C.-H. H. Chu is with the Center for Advanced Computer Studies, University of Southwestern Louisiana, Lafayette, LA 70504.

E. J. Delp is with the Computer Vision and Image Processing Laboratory, School of Electrical Engineering, Purdue University, West Lafayette, IN 47907.

IEEE Log Number 8825100.

II. Morphological Operators

Mathematical morphology, which is based on set operations, provides an approach to the development of nonlinear signal processing operators that incorporate shape information of a signal [10]. In mathematical morphological operations, the result of a set transformed by another set depends on the shapes of the two sets involved. The *shape* of a signal is determined by the values that the signal takes on. The shape information of the signal is extracted by using a *structuring element* to operate on the signal.

Morphological operators were developed in the image processing field for machine vision and medical imaging applications [11]. Morphological operators have been used in a limited way for background normalization of biological signals [12]. Operators that are used to process the EKG data for noise suppression and background normalization as described in this paper are known in the image processing literature as gray-scale morphological operators [11]. There are two basic morphological operators: erosion and dilation. These operators are usually applied in tandem; opening and closing are two derived operations defined in terms of erosion and dilation. These operators are described in detail below.

A. Erosion and Dilation

Throughout this section, f and k denote two discrete functions defined on $F = \{0, 1, \cdots, N-1\}$ and $K = \{0, 1, \cdots, M-1\}$, respectively; i.e., $f: F \rightarrow \boldsymbol{I}$ and $k: K \rightarrow \boldsymbol{I}$ where $\boldsymbol{I}$ denotes the set of integers. It is further assumed that $N > M$.

0018-9294/89/0200-0262$01.00

The *erosion*[1] of a function f by another function k, which we shall call the structuring element, denoted $f \ominus k$, is defined as

$$(f \ominus k)(m) = \min_{n=0,\cdots,M-1} f(m+n) - k(n),$$

$$\text{for } m = 0, \cdots, N-M.$$

Erosion is a "shrinking" operator in that values of $f \ominus k$ are always less than those of f. To determine the value of $f \ominus k$ at a point m, the procedure is to

1) translate the structuring element to m,

2) subtract the structuring element from the input signal, and

3) find the minimum value of the differences.

An example of erosion is shown in Fig. 1. The structuring element has a length of 3 and a constant value of 1. The original data consist of a sinusoidal signal corrupted by unwanted impulsive notches. The data are shown marked with squares while the result after erosion is shown marked with circles.

The *dilation*[2] of f by k, $f \oplus k$, is defined as

$$(f \oplus k)(m) = \max_{n=m-M+1,\cdots,m} f(n) + k(m-n),$$

$$\text{for } m = M-1, M, \cdots, N-1.$$

The dilation operation is an "expansion" operation in that the values of $f \oplus k$ are always greater than those of f. The procedure to determine the value of $f \oplus k$ at m is to

1) left-right reverse the structuring element k,

2) translate the reversed structuring element to m,

3) add the reversed structuring element to the input signal, and

4) find the maximum value of the sums.

An example of dilation is shown in Fig. 1. The structuring element has a length of 3 and a constant value of 1, the same as the one used in the previous example of erosion. The signal shown marked with circles is being dilated and the result after dilation is shown marked with triangles.

The complexity of an erosion or a dilation is comparable to that of discrete convolution. The role of the structuring element is analogous to that of the window kernel of a convolution. Within the window defined by the structuring element, instead of performing a pointwise multiplication, pointwise subtraction or addition is performed. The resulting value for that window is determined by a minimization or maximization instead of a summation.

B. Opening and Closing

The two basic operations, erosion and dilation, are usually applied in tandem. Opening and closing are two operations defined in terms of the basic operations. *Opening* of a data sequence by a structuring element is defined as erosion followed by a dilation. *Closing* of a data sequence by a structuring element is defined as dilation followed by an erosion. The opening of a data sequence can be interpreted as sliding the structuring element along the data sequence from beneath and the result is the highest points reached by any part of the structuring element. Similarly, the closing of a data sequence can be interpreted as sliding a "flipped-over" version of the structuring element along the data sequence from above and the result is the lowest points reached by any part of the structuring element.

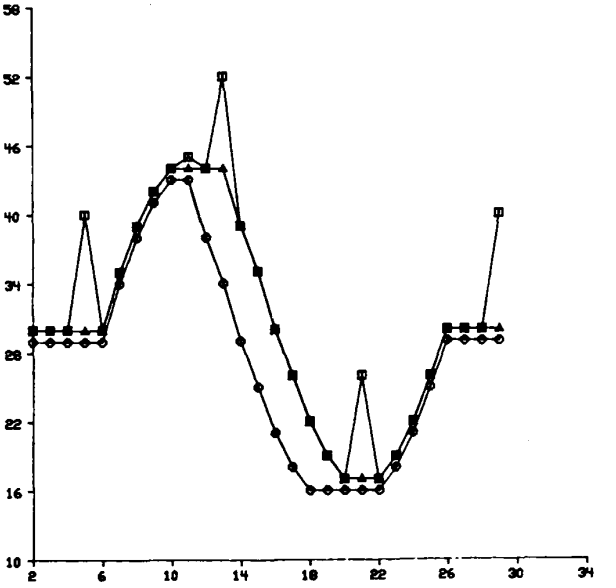

Fig. 1. Example of morphological operators. The structuring element k has length 3 and a constant value of 1. The original input signal f consists of a sine wave corrupted by impulsive noise. f is marked with squares; the eroded signal $f \ominus k$ is marked with circles. The eroded signal is then dilated to form $(f \ominus k) \oplus k$, which is marked with triangles. Together, the erosion followed by dilation is an opening operation.

It can be seen then that the shape of the output of either opening or closing is affected by the shape of the structuring element. Depending on the shape characteristics of the signal that is to be preserved, a specific structuring element has to be designed for processing the data. In most applications, opening is used to suppress peaks while closing is used to suppress pits. For example, the result of opening any sequence with a structuring element that is flat and has a length of M will not contain any peak within any interval of length $M-1$; while the result of closing any sequence with such a structuring element will not contain any pit within any interval of length $M-1$.

Noting that an opening operation is an erosion followed by a dilation, the examples of erosion and dilation described above can be seen as the two steps that make up an opening operation example. The original data sequence formed by a sinusoidal signal corrupted by impulsive noise is shown in Fig. 1 marked with squares. This data sequence was eroded and dilated by the same structuring element that has length 3 and a constant value of 1. The result after opening, with the spurious peaks

[1]This definition of erosion is commonly known as gray-scale erosion in the literature.

[2]This definition of dilation is commonly known as gray-scale dilation in the literature.

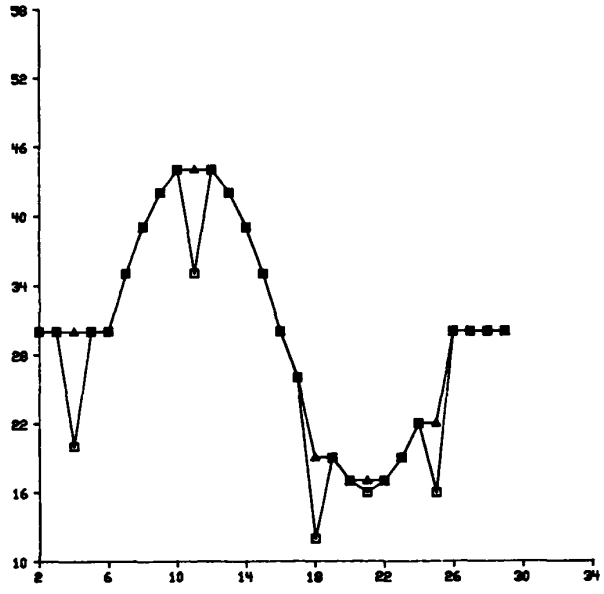

Fig. 2. Example of closing. The structuring element k has length 3 and a constant value of 1. The original input signal g consists of a sine wave corrupted by negative impulsive noise. g is marked with squares; the result after closing $(g \oplus k) \ominus k$ is marked with triangles.

suppressed, is shown in Fig. 1 marked with triangles. Fig. 2 shows an example of applying the closing operation to a data sequence formed by a sinusoidal signal corrupted by negative impulsive spikes. The original signal is shown marked with squares while the result after closing is shown marked with triangles. It can be seen that the negative impulsive peaks are removed by the closing operation.

III. A New Algorithm

The algorithm uses two steps to process the EKG signal: 1) impulsive noise suppression, and 2) background normalization. The block diagram of the algorithm is shown in Fig. 3.

Impulsive noise suppression is performed by processing the data through a sequence of opening and closing operations. The EKG signal, as well as any baseline drift, is estimated by processing the data using an opening operation followed by a closing operation. A second estimate of the signal is formed by processing the data using a closing operation followed by an opening operation. The result from this step is the average of the two estimates. If the amount of processing is a concern, either branch of the block diagram can be deleted with some performance degradation.

The design of the structuring element depends on the shape of the signal that is to be preserved. Since the opening and closing operations are intended to remove impulses, the structuring element must be designed so that the waves in the EKG signal are not removed by the process. A structuring element is characterized by its "shape," width, and height. Its width, or length, is largely determined by the duration of the major waves and the sampling rate. Denoting the duration of one of the waves as T sec, and the sampling rate as S Hz, the number

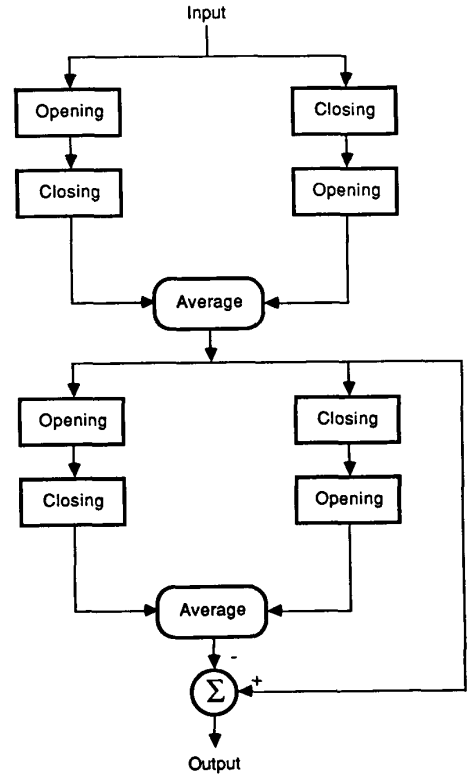

Fig. 3. Block diagram of the algorithm for suppressing impulsive noise and normalizing background drift.

of samples that correspond to a wave is then $T \times S$. Thus, the length of the structuring element must be less than $T \times S$.

The values of the structuring element determines the shape of the output waveform. Since in practice the EKG signal is not an ideal deterministic signal, we can only loosely classify the shape of its waves as triangular or dome-like. Due to this imprecise classification, the structuring element in practice has to be a lot shorter than $T \times S$ samples. Many structuring element implementations with the same width and height can be classified as dome-like. In Section VI, a dome-like structuring element model parameterized by its width, height, and "shape" is used to examine how each of the parameters affects the noise suppression performance of the algorithm.

Background normalization is performed by estimating the drift in the background and subtracting it from the incoming data. The background drift is estimated by removing the EKG signal from the data. The data are first opened by a structuring element that removes peaks which results in a pit where the EKG signal is located. This pit is removed by a closing operation using a larger structuring element. The result is then an estimate of the baseline drift.

In this step, two structuring elements are used: one for removing peaks and the other for removing the pit left after the previous operation. The design of the first structuring element is determined by the duration of the waves in the EKG signal. As in the previous discussion, denote

the duration of one of the waves by T sec, and the sampling rate by S Hz, the number of samples of a wave is $T \times S$. To remove the wave, a structuring element must have its length L greater than $T \times S$. The second structuring element is used to remove the pit left by the first operation, thus its length must be roughly $2L$.

A second estimate can be made by first closing the data by a structuring element which results in a hump where the EKG signal is located, followed by an opening operation using a larger structuring element. The two estimates are then averaged to form the baseline drift estimate. Correction of the baseline roll and drift is then done by subtracting the baseline drift estimate from the result obtained from the previous step.

IV. Experiments with a Known Signal

A number of experiments were performed using test data formed by adding impulsive noise and baseline drift to a signal digitized from an analog EKG simulator. This is done so that the algorithm could be tested in an absolutely controlled environment. Using a corrupted known signal as test data allows the performance of the algorithm to be evaluated by comparing the recovered signal with the known signal. Moreover, the degree of corruption of the input data can be seen, in part, by considering the difference between the data before and after the corruption.

A noisy sequence of EKG data is modeled as

$$r(n) = s(n) + i(n) + b(n)$$

where $s(n)$ is the signal that includes the *QRS* waves, $i(n)$ is the noise component, and $b(n)$ is the baseline drift.

Signal: A known EKG signal was obtained from a FOGG Model M310 ECG Simulator that generates a signal with 5 mV amplitude. The signal was sampled at 1 kHz and quantized to 12 bits (i.e., the digitized sample values range from -2048 to 2047). The maximum and minimum values of the EKG signal are 1636 and -1722, respectively. Fig. 4 shows a sequence of the digitized EKG signal with the rate at 100 beats per min. The unit of the time axis in Fig. 4 is $1/1000$ s.

Noise: Impulsive noise is generated by an ϵ mixture of Gaussian noise that has a probability distribution function of

$$P_i(y) = (1 - \epsilon)\,\Phi\left(\frac{y}{\sigma_1}\right) + \epsilon\Phi\left(\frac{y}{\sigma_2}\right)$$

where $\Phi(y)$ is the probability distribution function of a Gaussian random variable with zero mean and unit variance. σ_2 is typically much larger than σ_1. With probability $(1 - \epsilon)$, the noise for sample $i(n)$ is a Gaussian random variable with standard deviation σ_1, which simulates the background noise; with probability ϵ, $i(n)$ is Gaussian with standard deviation σ_2, which simulates the impulsive noise. As σ_1 and σ_2 increases, the noise amplitude increases. As ϵ increases, the frequency of impulse noise occurrence increases. A sample of such a noise sequence with $\epsilon = 0.2$, $\sigma_1 = 65$, and $\sigma_2 = 650$ is shown in Fig. 5.

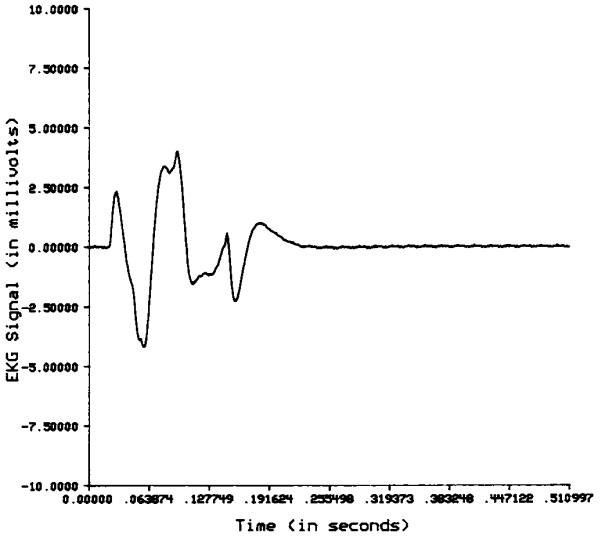

Fig. 4. A digitized EKG signal sequence from the analog EKG simulator.

Baseline Drift: The baseline drift is simulated by adding a slanted line to a sinusoid:

$$b(n) = B + m \times n + A \times \cos\left(2\pi\frac{n}{N} + \phi\right).$$

The period of the sinusoid N controls the severity of the baseline roll while the slope of the line m controls the degree of upward or downward drift. Using different values for ϕ allows different baseline drift sequences to be generated with similar characteristics. The bias term B is set so that the sequence values do not get out of range. Figs. 6 and 7 show test data formed by adding an EKG signal to impulsive noise and a baseline drift sequence.

Performance Measures: Three metrics were used to measure the difference between two signals s and $\hat{s}$ assuming they each have L of points:

$$d_1(s, \hat{s}) = \frac{1}{R}\frac{1}{L}\sum_{n=1}^{L}\left|s(n) - \hat{s}(n)\right|,$$

$$d_2(s, \hat{s}) = \frac{1}{R}\left\{\frac{1}{L}\sum_{n=1}^{L}\left|s(n) - \hat{s}(n)\right|\right\}^{1/2},$$

$$d_\infty(s, \hat{s}) = \frac{1}{R}\max_{n=1,\cdots,L}\left|s(n) - \hat{s}(n)\right|.$$

d_2 is a measure of the root-mean-squared difference between two signals and is the most commonly used metric. d_1 is a measure of the mean absolute difference while d_∞ is a measure of the maximum deviation of one signal from another. They are normalized by R, the peak-to-peak value of s.

A. Test Results

Data sequences corrupted using different sets of noise parameters were used to test the algorithm. Throughout

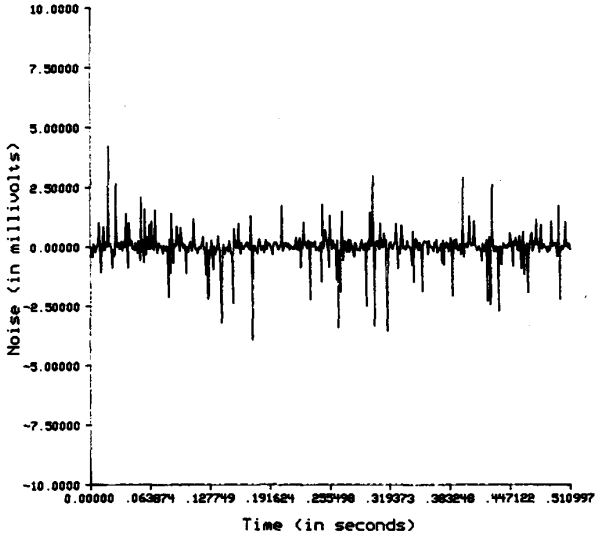

Fig. 5. A sample noise sequence. The noise parameters are: $\epsilon = 0.2$, $\sigma_2 = 650$, and $\sigma_1 = 65$.

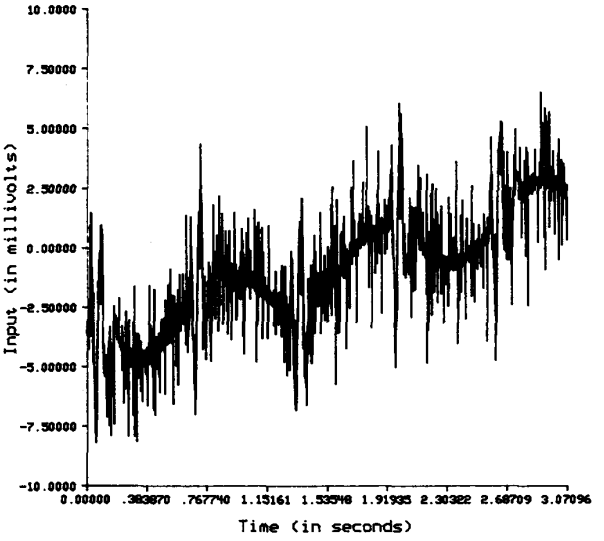

Fig. 7. An EKG signal corrupted by additive noise and baseline drift (3072 data points shown).

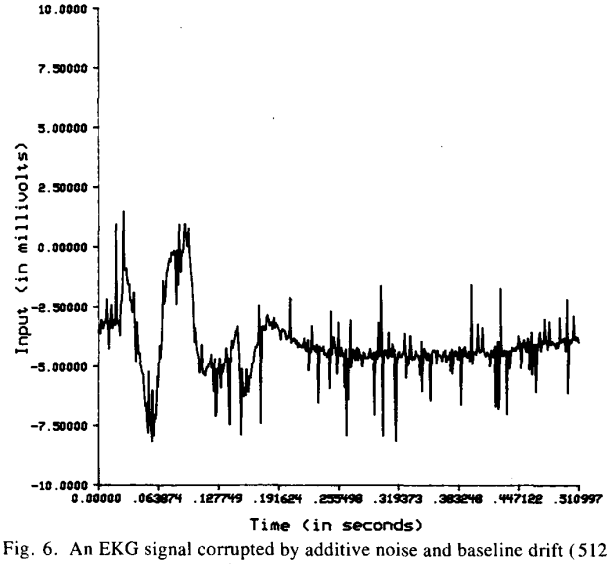

Fig. 6. An EKG signal corrupted by additive noise and baseline drift (512 data points shown).

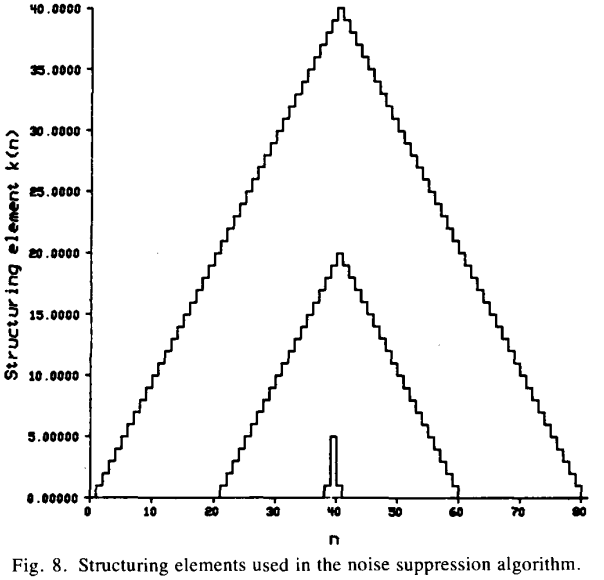

Fig. 8. Structuring elements used in the noise suppression algorithm.

this section, $s(n)$ denotes the noiseless EKG signal, $r(n)$ denotes the corrupted data, and $\hat{s}(n)$ denotes the processed result.

The structuring element used for noise suppression has length 5 and values of (0, 1, 5, 1, 0). The structuring element used in the first stage of background normalization has a triangular shape and length 41. The second structuring element also has a triangular shape and has length 81. These structuring elements are shown in Fig. 8.

For the input data sequence depicted in Figs. 6 and 7, the parameters are

ϵ mixture noise: $\epsilon = 0.2$, $\sigma_1 = 65$ and $\sigma_2 = 650$,

baseline drift: $m = 0.8$, $A = 500$, $N = 1000$

Based on 3000 data points, the differences between s and r as measured by the three metrics are

$$d_1(s, r) = 0.2433,$$

$$d_2(s, r) = 0.2993,\ d_\infty(s, r) = 0.9887.$$

Results of applying the new algorithm to this signal are shown in Figs. 9 and 10. Fig. 9 shows 512 points of the output, indicating the noise suppression performance. Fig. 10 shows 3072 points of the same output sequence, illustrating the baseline correction capability of the algorithm. The performance measures calculated based on 3000 data points are

$$d_1(s, \hat{s}) = 0.02652,$$

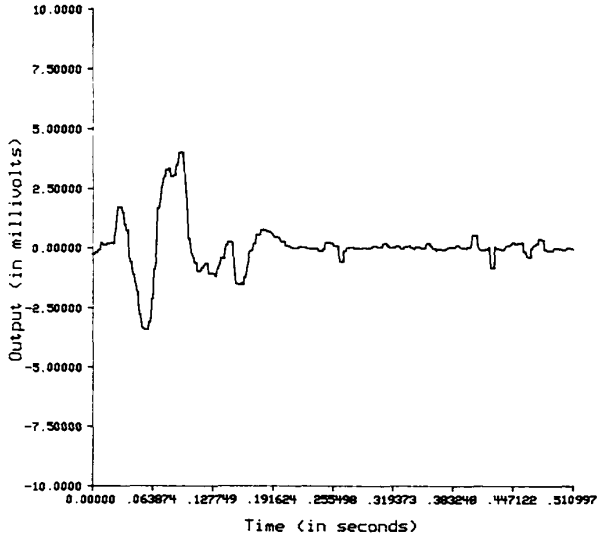

Fig. 9. Result after processing the input data shown in Fig. 6 (512 data points shown).

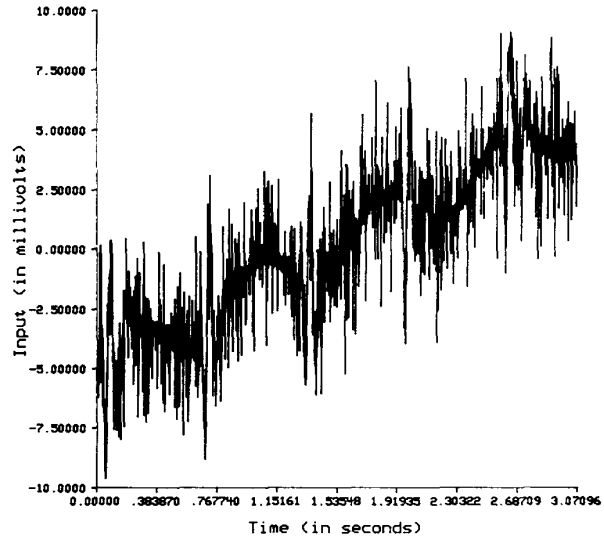

Fig. 11. An EKG signal corrupted by additive noise and baseline drift (3072 data points shown).

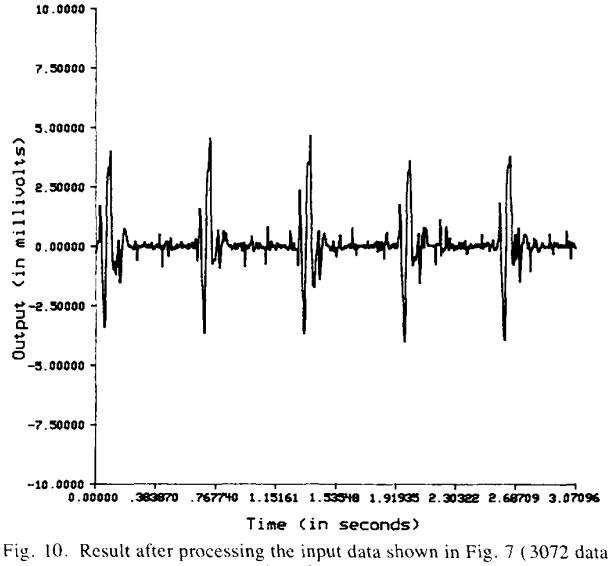

Fig. 10. Result after processing the input data shown in Fig. 7 (3072 data points shown).

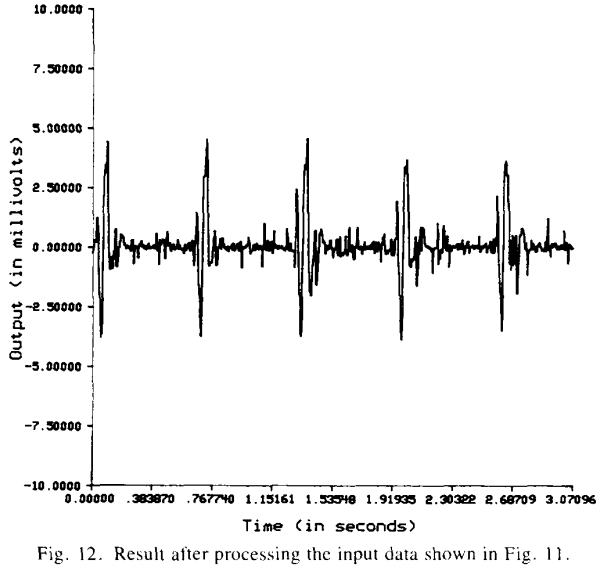

Fig. 12. Result after processing the input data shown in Fig. 11.

As measured by d_2, the input data deviates from the signal by 30 percent of the peak-to-peak signal value. This value is a measure of the power of the noise and the baseline drift. The deviation was reduced to 4 percent by the processing.

A different set of noise parameters that increases the noise level and baseline drift was used to corrupt the signal shown in Fig. 11; the parameters for this signal are

ϵ mixture noise: $\epsilon = 0.25$, $\sigma_1 = 75$ and $\sigma_2 = 750$

baseline drift: $m = 1.4$, $A = 500$, $N = 800$

and $\phi = 0.3$.

Based on 3000 data points, the differences between s and r as measured by the three metrics are

$$d_1(s, r) = 0.3358,$$

$$d_2(s, r) = 0.3922,\ d_\infty(s, r) = 1.10155.$$

Results of applying the algorithm to this signal is shown in Fig. 12. The performance measures were calculated based on 3000 data points to be

$$d_1(s, \hat{s}) = 0.03087,$$

$$d_2(s, \hat{s}) = 0.04506,\ d_\infty(s, \hat{s}) = 0.2281.$$

Compared to the previous experiment, the noise and baseline drift power was increased to 40 percent of the peak-to-peak signal value. The result after processing still achieves a low 4.5 percent deviation.

The effectiveness of the new algorithm in suppressing

noise and correcting baseline drift and roll can be seen through the empirical performance measures and by plots of the results. In the next section, the noise suppression performance of the algorithm under a wider range of situations will be examined.

V. Noise Suppression Performance

The structuring element with length 5 and values (0, 1, 5, 1, 0) was used to study the noise suppression of the algorithm under a variety of noise situations. Noise as modeled in Section IV was used; the EKG signal was corrupted by noise with different ϵ and σ_2/σ_1 values. The value of ϵ ranged from 0.1 to 0.5, corresponding to an increasing probability of impulsive noise occurrence. At $\epsilon = 0.5$, a sample has equal probability of being corrupted by background Gaussian noise or by higher amplitude impulsive noise. The standard deviation of background Gaussian noise σ_1 was set at 65. The standard deviation of impulsive Gaussian noise σ_2 ranged from $2\sigma_1$ to $20\sigma_1$, corresponding to the increasing impulse amplitudes. To consider the severity of the impulsive noise, recall that the peak values of the EKG waves are 1636 and -1772. At $\sigma_2 = 650$, the impulsive noise amplitude is above 1300 with probability 4.5 percent. At $\sigma_2 = 1300$, the impulsive noise amplitude is above 1300 with probability 31.7 percent. The resulting values of the performance measure d_2 are shown in Fig. 13. The minimum d_2 value 0.01248 was recorded for $\epsilon = 0.1$ and $\sigma_2 = 130$. The maximum d_2 value 0.11024 was recorded for $\epsilon = 0.5$ and $\sigma_2 = 1300$, which corresponds to the case with the largest amount of noise. As can be seen from Fig. 18, as the noise situation worsens, the performance deteriorates very gradually and exhibits no abrupt jumps or sharp rises.

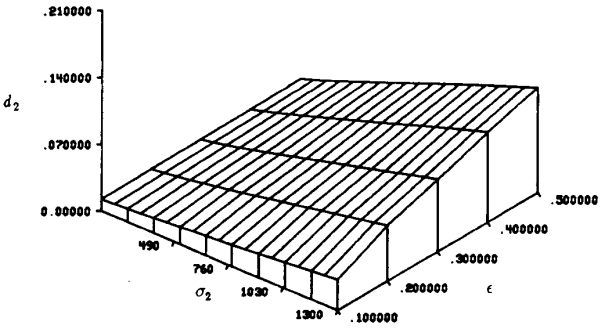

Fig. 13. Noise suppression performance as measured by d_2 for different values of ϵ and σ_2. σ_1 was set at 65.

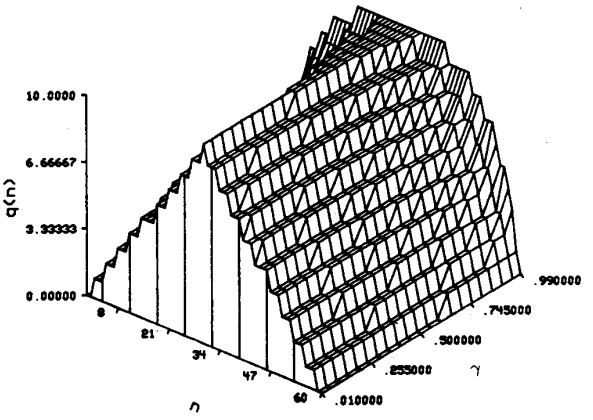

Fig. 14. Structuring elements with different γ values.

VI. Experiments with a Parameterized Structuring Element

Unlike the design of linear filters, methods for structuring element design in morphological signal processing is an open research problem [13]. In this section, we use a dome-like structuring element parameterized by its width, height, and "shape" to examine these effects on the noise suppression performance of the algorithm. The parametric structuring element is denoted by $q(n)$, for $n = 0, 1, \cdots, 2N$. N is the parameter that determines the width of q. For $n = 0, 1, \cdots, N$, let

$$q(n) = h \times (1 - e^{-\alpha n}),$$

and for $n = N + 1, \cdots, 2N$, let

$$q(n) = q(2N - n).$$

The structuring element q is then symmetric with respect to the peak at $q(N)$. The height of q is controlled by h; the actual height parameter we used is the peak value of $q(N)$, which is a function of h. The "shape" of q is controlled by α, which ranges from 0 to ∞. The parameter that we used instead is γ, which ranges from 0 to 1; γ is related to α by

$$\gamma = 1 - e^{-\alpha N}.$$

As γ increases, q changes from thick and round to thin and sharp. Fig. 14 shows a plot of q with γ varying from 0.01 to 0.99. To illustrate the shape change, the peak value $q(N)$ was set at 10 while the width parameter N was set at 30.

The parametric structuring element with different sets of parameters was used in the noise suppression stage of the algorithm to process the known signal corrupted by impulsive noise as described in Section IV. The parameters for the ϵ mixture noise are $\epsilon = 0.2$, $\sigma_1 = 65$, and $\sigma_2 = 650$. The different parameter values for the structuring element used were

γ:	0.99, 0.9, 0.8, 0.7, 0.6, 0.5, 0.4, 0.3, 0.2, 0.1;
$q(N)$:	1, 3, 5, 7, 9, 11, 13, 15, 17, 19;
N:	1, 3, 5, 7, 9, 11, 13, 15, 17, 19.

The performance was evaluated by comparing the input to the output relative to the d_2 metric. From the results, the only parameter that has a significant effect on the performance is the width. Fig. 15 shows the result for N fixed

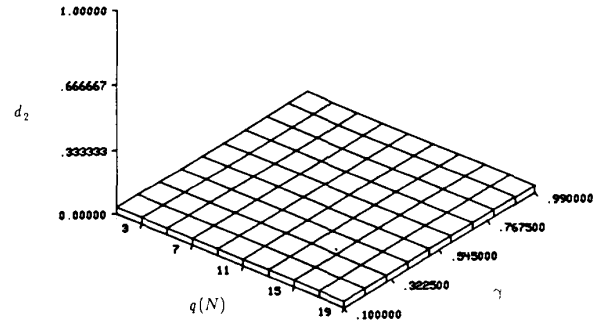

Fig. 15. Noise suppression performance as measured by d_2 of the parametric structuring element with N set at 3.

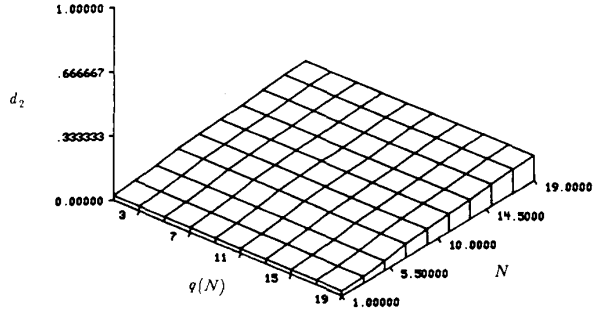

Fig. 16. Noise suppression performance as measured by d_2 of the parametric structuring element with γ set at 0.5.

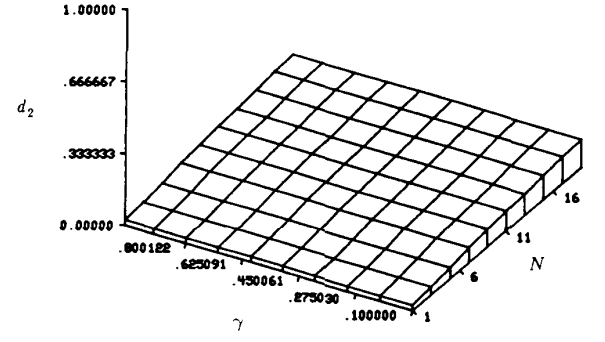

Fig. 17. Noise suppression performance as measured by d_2 of the parametric structuring element with $q(N)$ set at 5.

at 3. It can be seen that the performance shows no significant change with different values of $q(N)$ and γ. Since there is not a lot of difference between structuring elements with different γ values when the width is as low as 7, it is understandable that γ does not affect the performance. We show results for $N = 3$ because it achieves a performance of $d_2 < 0.03$, compared with 0.09 which is how much the input data deviates from the signal. Fig. 16 shows the result for γ fixed at 0.5. It can be seen that the performance deteriorates with increasing N but shows no change due to varying $q(N)$. Fig. 17 shows the result for $q(N) = 5$; again, it can be seen that the performance deteriorates with increasing N but shows no change due to varying γ.

VII. Sinusoidal Response

Guidelines have been established by the American Heart Association for EKG signal processing relative to acceptable frequency response of linear filters [14]. It is difficult, however, to show that the algorithm described in this paper conforms to these guidelines because nonlinear filtering cannot be analyzed in terms of frequency response. Linear filtering, via the superposition principle, allows frequency response analysis by decomposing the input and output into a sum of sinusoidals. The superposition principle does not apply to nonlinear filters; hence, "bandwidth" is a meaningless quantity. There is ongoing work in the theoretial analysis of morphological operators based on a weaker form of the superposition principle, known as threshold decomposition [15], [8]. The general problem of investigating the response of morphological operators to a sinusoidal input remains an open research problem [16]. In this section, we address this problem by examining the sine-wave response of the new algorithm to study the extent that these signals are modified relative to the type of structuring element.

According to the American Heart Association committee report on electrocardiography [14], the recommended lower bound of amplitude frequency response is flat from 0.14 Hz to 50 Hz, reduced from unit gain by no more than 6 percent. Since morphological processing is discrete in nature, if a sinusoidal signal with a certain frequency is unmodified, any signals with a lower frequency would also be unmodified. Sinusoidal signals at frequencies ranging from 0 Hz to 180 Hz, sampled at rates ranging from 360 Hz to 1800 Hz were processed by the noise suppression algorithm using the five-element structuring element shown in Fig. 8. The processed result is compared to the original sinusoidals using the d_2 performance measure described in Section IV and is shown in Fig. 18. The values for d_1 and d_∞ show similar characteristics. The performance measure shows a steady rise as the sampling rate drops and as the input frequency increases, up to a point where it flats out.

It should be emphasized that there is no direct relation between these plots and the common amplitude frequency response plot used to describe linear filters. As the results indicate, increasing the sampling rate produces better results. For example, a sampling rate in the range of 1000 Hz is needed to obtain performance that achieves $d_2 < 0.10$ for input with a frequency of up to 50 Hz, which is the upper frequency limit for the flat response required by the American Heart Association for "faithful reproduction of the electrocardiographic waveform" [14]. It is difficult to set a general performance standard since it depends on other factors such as the intended application of the processed data. The choice of 0.1 here is based on the

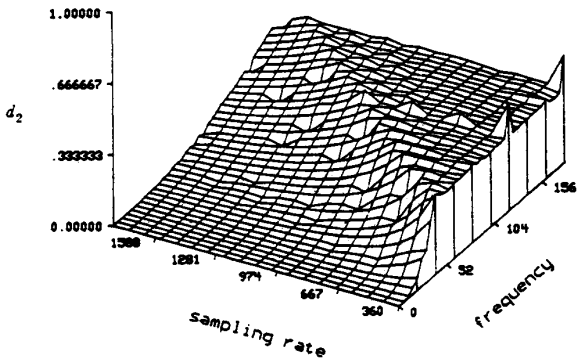

Fig. 18. Amount of modification of sampled sinusoidal input as measured by d_2 plotted against input frequencies and sampling rates.

observation that for a fixed sampling rate, d_2 tends to rise relatively quickly after it reaches 0.1.

Since the processing is discrete, the signal bandwidth, the sampling rate, and the structuring element length are all related. The highest frequency of the signal is usually dictated by the application: e.g., 50 Hz in EKG signal processing. Given that the signal frequency is fixed, either the structuring element can be shortened or a higher sampling rate can be used to minimize the distortion of the waveform. The minimum length of the structuring element is determined by the nature and characteristics of noise expected. For example, for impulsive noise, a typical choice of the minimum length is from 3 to 5; for other artifact suppression, the minimum length might have to be increased depending on the situation.

The problem is examined below from the viewpoint of determining the required sampling rate of the EKG data for a given required performance. A structuring element with length $2N + 1$ modifies a wave of an EKG signal by truncating its top. The worst case is for a structuring element to have a constant value of 0. Let the tolerated attenuation factor be $1 - \tau$; i.e., the tip of the wave should not be truncated by a factor more than τ. Suppose we model a wave by a raised cosine waveform with frequency f_0 Hz. A reasonable estimate of f_0 is 50 since it then follows that the duration of a wave is 20 ms. Typically, a *QRS* complex with three waves lasts from 80 to 100 ms. It can easily be shown that the sampling rate f_s is given

$$f_s = \frac{2\pi f_0 N}{\cos^{-1}(1 - \tau)}. \tag{1}$$

For example, with $N = 2$, $f_0 = 50$ Hz, and $\tau = 0.06$, we found f_s to be 1.8 kHz.

Alternatively, we can model a wave by a Gaussian pulse with σ^2 as its variance. Denoting the bandwidth of the signal as f_0 Hz, and noting that the Fourier transform of a Gaussian pulse is a Gaussian pulse with variance $(2\pi\sigma)^{-2}$, we see that the sampling rate f_s can be determined by

$$f_s = \frac{2\pi f_0 N}{\left(-2 \log (1 - \tau)\right)^{1/2}}. \tag{2}$$

Using $\tau = 0.06$, $f_0 = 50$ Hz, $N = 2$, we again obtain f_s as 1.8 kHz. From (1) and (2), we see that the required sampling rate varies directly with N and f_0. It varies inversely and nonlinearly with τ. Consequently, as τ increases, f_s decreases rather rapidly.

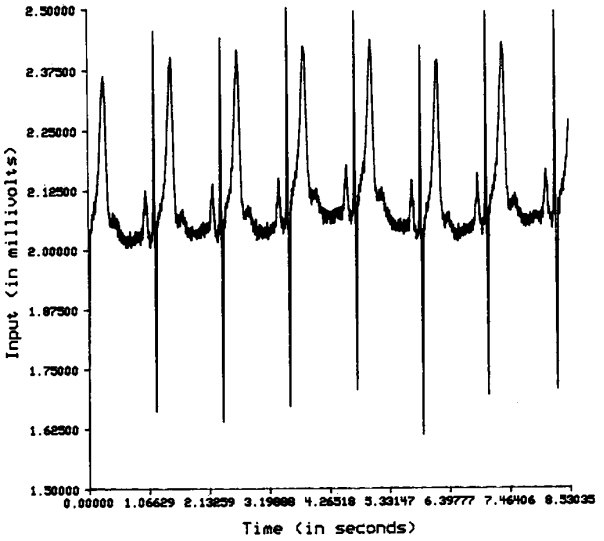

Fig. 19. A sequence of EKG signal classified as "of excellent quality" from tape 117 of the MIT-BIH database.

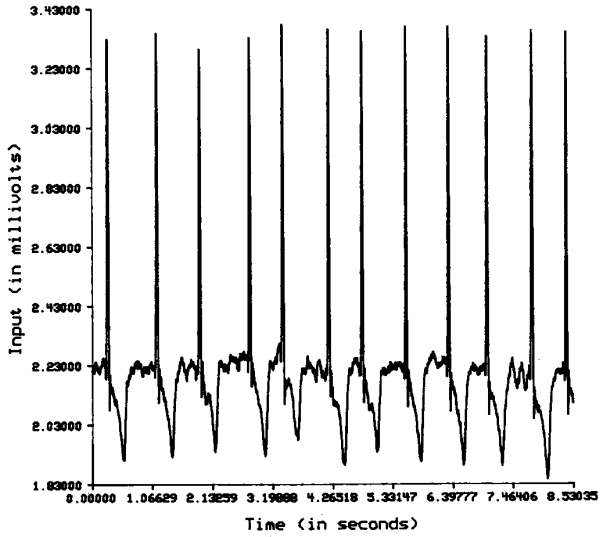

Fig. 20. A sequence of EKG signal classified as "of excellent quality" from tape 219 of the MIT-BIH database.

VIII. Experiments with Real EKG Signals

EKG data from the MIT-BIH arrhythmia database [17] were used to evaluate the algorithm performance. Each

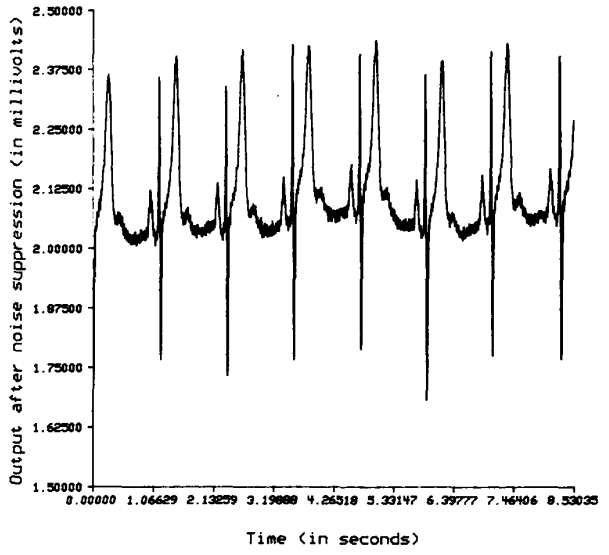

Fig. 21. Result of noise suppression on the data sequence shown in Fig. 19.

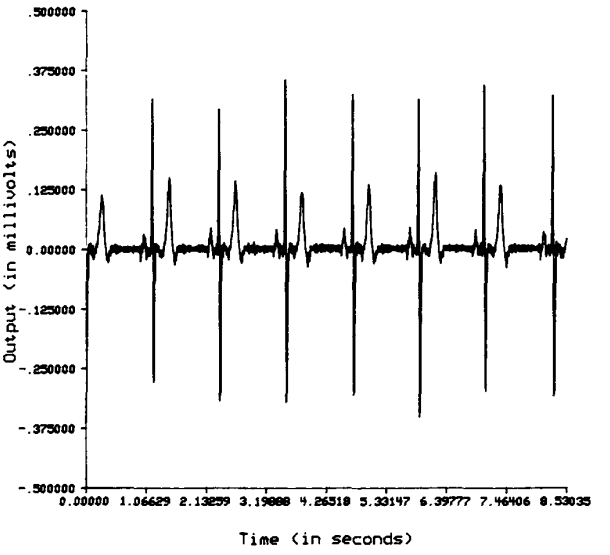

Fig. 23. Result after baseline correction and noise suppression on the data sequence shown in Fig. 19.

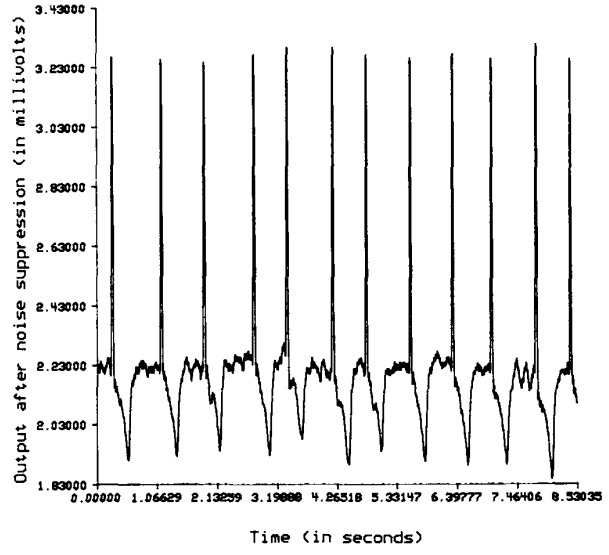

Fig. 22. Result of noise suppression on the data sequence shown in Fig. 20.

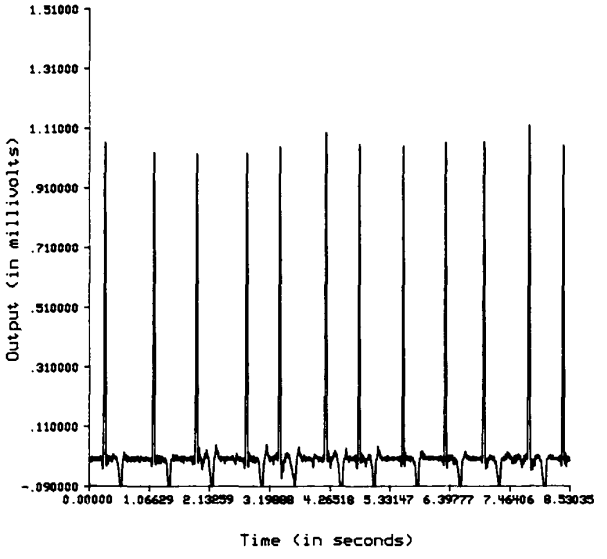

Fig. 24. Result after baseline correction and noise suppression on the data sequence shown in Fig. 20.

set of data was digitized at 360 Hz without interruption from a single patient using a modified EKG "lead 2" in which electrodes were placed at the right shoulder and the left abdomen of the patient [17].

The processing is done using the structuring elements shown in Fig. 8. The unit of time axis for the plots shown in Figs. 19 to 26 is 1/360 s. Figs. 19 and 20 show two sequences that were considered to be of "excellent quality" (tapes 117 and 219 of the MIT-BIH database). Figs. 21 and 22 show the result after noise suppression processing, the original signal is not significantly modified. Figs. 23 and 24 show the result after background normalization, the original signal is modified to some degree, most notably in the areas of the ST segment. Due to the nature of background normalization, the reference level of the signal is also biased to zero.

Fig. 25 shows a signal exhibiting bursts of "baseline wander" (tape 111 of the MIT-BIH database). Fig. 26 shows the result after processing. Again, we see very slight modification of the signal, but the background drift is corrected. The reference level of the signal is also biased to zero.

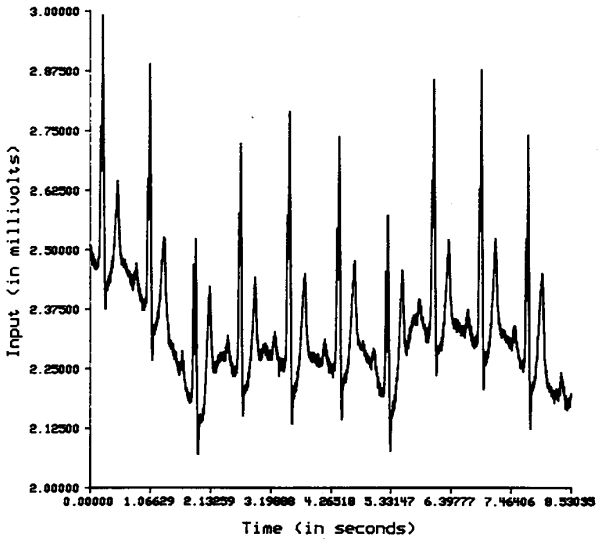

Fig. 25. A sequence of EKG signal showing baseline wander from tape 111 of the MIT-BIH database.

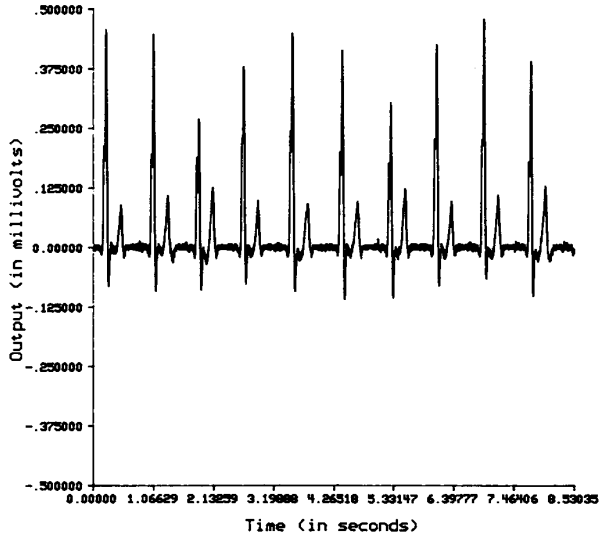

Fig. 26. Result after baseline correction and noise suppression on the data sequence shown in Fig. 25.

IX. Concluding Remarks

A new approach to EKG signal processing has been presented using mathematical morphological operators. The effectiveness of the new algorithm in impulsive noise suppression and background normalization was first demonstrated by using a corrupted known signal and measuring the difference between the known signal and the processed result. The performance was further examined by processing clinically acquired EKG data from a standard set. The effect of the algorithm was tested on acquired EKG signals classified by experts to be "of excellent quality." A comparison of the original signal, the result after noise suppression, and the result after baseline correction shows that the modification is due mostly to baseline correction.

The performance of the algorithm is dependent on three related factors: amount of noise, choice of structuring element, and sampling rate of the signal. Results in Section V show that a five-element structuring element can handle a large amount of impulsive noise. The results in Section VI indicate that the length of the structuring element plays a more important role, compared to either the height or the shape, in determining the noise suppression performance. This result is consistent with the use of median filters relative to EKG data [18]. The algorithm described in this paper is currently undergoing clinical testing at the University of Michigan Medical School.

Morphological signal processing is an area that is receiving increasing attention. In this paper, we have considered the signal processing aspects of these operators that are important relative to their application to EKG signals. Morphological operators are also attractive for their relatively simple computational demands: the computation is made up of addition, subtraction, and logical comparison. It has been shown that these types of algorithms can be implemented in VLSI for real-time processing [19]. While morphological operators have not yet been as widely used in one-dimensional signal processing as in image processing, they seem particularly well suited for processing EKG data since the signal components are well characterized by their shapes.

Acknowledgment

We are indebted to Dr. A. J. Buda of the Cardiology Division, University of Michigan Medical School, for his help and criticism in the development of the algorithm and its testing on clinical data. We would like to thank the reviewers for their comments and suggestions; we would further like to thank Major B. J. Stanton of the U.S. Air Force Academy and Prof. S. C. Bass of Purdue University for their help and suggestions.

References

[1] G. B. Moody, W. K. Muldrow, and R. G. Mark, "A noise stress test for arrhythmia detectors," in *Computers in Cardiology*. 1984, pp. 381-384.

[2] M. L. Ahlstrom and W. J. Tompkins, "Digital filters for real-time ECG signal processing using microprocessors," *IEEE Trans. Biomed. Eng.*, vol. BME-32, pp. 708-713, Sept. 1985.

[3] O. Pahlm and L. Sornmo, "Data processing of exercise ECG's," *IEEE Trans. Biomed. Eng.*, vol. BME-34, pp. 158-165, Feb. 1987.

[4] J. Wartak, *Computers in Electrocardiography*. Springfield, IL: Thomas, 1970.

[5] O. Pahlm and L. Sornmo, "Software *QRS* detection in ambulatory monitoring—A review," *Med. Biol. Eng. Comput.*, vol. 22, pp. 289-297, July 1984.

[6] J. A. van Alste and T. S. Schilder, "Removal of baseline wander and power-line interference from the ECG by an efficient FIR filter with a reduced number of taps," *IEEE Trans. Biomed. Eng.*, vol. BME-32, pp. 1052-1060, Dec. 1985.

[7] N. C. Gallagher and G. L. Wise, "A theoretical analysis of the properties of median filters," *IEEE Trans. Acoust., Speech, Signal Processing*, vol. ASSP-29, pp. 1136-1141, Dec. 1981.

[8] P. D. Wendt, E. J. Coyle, and N. C. Gallagher, "Stack filters," *IEEE Trans. Acoust., Speech, Signal Processing*, vol. ASSP-34, pp. 898-911, Aug. 1986.

[9] P. Maragos and R. W. Schafer, "Morphological filters—Part I: Their set-theoretic analysis and relations to linear shift-invariant filters," *IEEE Trans. Acoust., Speech, Signal Processing*, vol. ASSP-35, pp. 1153–1169, Aug. 1987.

[10] J. Serra, *Image Analysis and Mathematical Morphology*. New York: Academic, 1982.

[11] R. M. Haralick, S. R. Sternberg, and X. Zhuang, "Image analysis using mathematical morphology: Part I," *IEEE Trans. Pattern Anal. Mach. Intell.*, vol. PAMI-9, pp. 532–550, July 1987.

[12] M. M. Skolnick and D. Butt, "Cellular array algorithms for the analysis of EKG signals," in *Proc. 1985 IEEE Workshop Computer Architectures Pattern Anal. Image Database Manage.*, Miami, FL, Nov. 1985, pp. 438–443.

[13] E. J. Coyle, "Rank order operators and the mean absolute error criterion," *IEEE Trans. Acoust., Speech, Signal Processing*, vol. 36, pp. 63–76, Jan. 1988.

[14] H. V. Pipberger, R. C. Arzbaecher, A. S. Berson, S. A. Briller, D. A. Brody, N. C. Flowers, D. B. Geselowitz, E. Lepeschkin, G. C. Oliver, O. H. Schmitt, and M. Spach, "Recommendations for standardization of leads and of specifications for instruments in electrocardiography and vectorcardiography: Report of the Committee on Electrocardiography, American Heart Association," *Circulation*, vol. 52, pp. 11–31, 1975.

[15] P. Maragos and R. W. Schafer, "Morphological filters—Part II: Their relations to median, order-statistic, and stack filters," *IEEE Trans. Acoust., Speech, Signal Processing*, vol. ASSP-35, pp. 1170–1184, Aug. 1987.

[16] J. Neejarvi, P. Heinonen, and Y. Neuvo, "Sine wave responses of median type filters," in *Proc. 1988 IEEE Internat. Symp. Circuits Syst.*, Helsinki, Finland, June 1988, pp. 1503–1506.

[17] Biomedical Engineering Center for Clinical Instrumentation, *MIT-BIH Arrhythmia Database Tape Directory and Format Specification*. Cambridge, MA: Harvard University–Massachusetts Institute of Technology, Division of Health Sciences and Technology, Oct. 1982.

[18] B. C. Yu, S. Liu, M. Lee, C. Y. Chen, and B. N. Chiang, "A nonlinear digital filter for cardiac *QRS* complex detection," *J. Clin. Eng.*, vol. 10, pp. 193–201, 1985.

[19] E. J. Coyle, "The theory and VLSI implementation of stack filters," in *VLSI Signal Processing II*. New York: IEEE Press, 1986.

Chee-Hung Henry Chu (M'86) received the B.S.E. (summa cum laude) degree in computer engineering in 1981, the M.S.E. degree in computer information and control engineering in 1982, both from the University of Michigan, Ann Arbor, MI, and the Ph.D. degree in electrical engineering from Purdue University, West Lafayette, IN, in 1988.

He is now an Assistant Professor of computer engineering at the Center for Advanced Computer Studies, University of Southwestern Louisiana, Lafayette, Louisiana. His research interests include signal processing and computer vision.

Dr. Chu is a member of the Optical Society of America, Association for Computing Machinery, Tau Beta Pi, and Eta Kappa Nu.

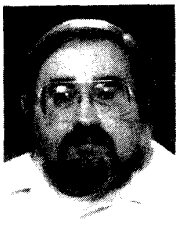

Edward J. Delp (S'70–M'79–SM'86) was born in Cincinnati, OH. He received the B.S.E.E. (cum laude) and M.S. degrees from the University of Cincinnati, Cincinnati, OH, in 1973 and 1975, respectively, and the Ph.D. degree from Purdue University, West Lafayette, IN, in 1979.

From 1980 to 1984, he was an Assistant Professor of Electrical and Computer Engineering at The University of Michigan, Ann Arbor. Since August 1984, he has been an Associate Professor of Electrical Engineering, Purdue University, West Lafayette, IN. His research interest lies in the broad area of communication and information theory but especially the transmission and processing of multidimensional signals. He has also consulted for various companies and government agencies in the areas of signal processing, robot vision, pattern recognition, and cryptography. He is a member of the editorial boards of the *International Journal of Cardiac Imaging* and the *Broadband Communications Journal*. He is also coeditor of the book *Digital Cardiac Imaging* (Martinus Nijhoff.)

Dr. Delp is a member of Tau Beta Pi, Eta Kappa Nu, Phi Kappa Phi, Sigma Xi, Optical Society of America, and Pattern Recognition Society.